Deep-Sea Research Part I 120 (2017) 14–28

Contents lists available at ScienceDirect

Deep–Sea Research I

journal homepage: www.elsevier.com/locate/dsri

Deep-sea coral and hardbottom habitats on the west Florida slope, eastern Gulf of Mexico

Steve W. Ross[a,*], Mike Rhode[a], Sandra Brooke[b]

[a] University of North Carolina at Wilmington, Center for Marine Science, 5600 Marvin Moss Ln, Wilmington, NC 28409, USA
[b] Florida State University, Coastal and Marine Laboratory, 3618 Coastal Hwy 98, St. Teresa, FL 32358, USA

ARTICLE INFO

Keywords:
Gulf of Mexico
West Florida slope
Deep-sea corals
Deep reefs
Lophelia pertusa
Habitat mapping
Loop Current

ABSTRACT

Until recently, benthic habitats dominated by deep-sea corals (DSC) appeared to be less extensive on the slope of the Gulf of Mexico (GOM) than in the northeast Atlantic Ocean or off the southeastern US. There are relatively few bioherms (i.e., coral-built mounds) in the northern GOM, and most DSCs are attached to existing hard substrata (e.g., authigenically formed carbonate). The primary structure-forming, DSC in the GOM is *Lophelia pertusa*, but structure is also provided by other living and dead scleractinians, antipatharians (black corals), octocorals (gorgonians, soft corals), hydrocorals and sponges, as well as abundant rocky substrata. The best development of DSCs in the GOM was previously documented within Viosca Knoll oil and gas lease blocks 826 and 862/906 (north-central GOM) and on the Campeche Bank (southern GOM in Mexican waters). This paper documents extensive deep reef ecosystems composed of DSC and rocky hard-bottom recently surveyed on the West Florida Slope (WFS, eastern GOM) during six research cruises (2008–2012). Using multibeam sonar, CTD casts, and video from underwater vehicles, we describe the physical and oceanographic characteristics of these deep reefs and provide size or area estimates of deep coral and hardground habitats. The multibeam sonar analyses revealed hundreds of mounds and ridges, some of which were subsequently surveyed using underwater vehicles. Mounds and ridges in < 525 m depths were usually capped with living coral colonies, dominated by *L. pertusa*. An extensive rocky scarp, running roughly north-south for at least 229 km, supported lower abundances of scleractinian corals than the mounds and ridges, despite an abundance of settlement substrata. Areal comparisons suggested that the WFS may exceed other parts of the GOM slope in extent of living deep coral coverage and other deep-reef habitat (dead coral and rock). The complex WFS region warrants additional studies to better understand the influences of oceanography and geology on the occurrence of DSC and associated organisms. Protection measures are being considered to ensure the long-term integrity of this diverse ecosystem.

1. Introduction

Until recently, benthic habitats dominated by deep-sea corals (DSC) appeared to be more scattered and less extensive in the Gulf of Mexico (GOM) (Brooke and Schroeder, 2007; Schroeder and Brooke, 2011) than on the slopes of the northeastern Atlantic Ocean (Hall-Spencer et al., 2007) or off the southeastern United States (SEUS) (Ross and Nizinski, 2007; Reed et al., 2013). In contrast with other regions of the North Atlantic, relatively few coral bioherms (elevations mostly created by successive coral growth, senescence and sedimentation) were known from the GOM slope, although extensive cold-water coral mounds were recently described from the Campeche Bank in the southern GOM (Hebbeln et al., 2014). Instead of building mounds, GOM DSCs were usually observed attached to abundant exposed hard substrata (Brooke and Schroeder, 2007), mostly authigenic carbonate blocks on the north-central GOM slope (Cordes et al., 2008; Schroeder and Brooke, 2011) and emergent carbonate and phosphorite hardgrounds on the slope of the eastern GOM (Brooks and Holmes, 2011). The main structure-forming DSC in the GOM is the branching scleractinian *Lophelia pertusa*, but complex structure is also provided by other living and dead scleractinians (e.g., *Madrepora oculata*, *Enallopsammia profunda*), antipatharians (e.g., *Leiopathes* sp.), octocorals (e.g., *Keratoisis flexibilis, Callogorgia americana*), hydrocorals (e.g., *Stylaster* sp.) and sponges, as well as the non-living rocky substrata (Schroeder and Brooke, 2011). Whether composed mostly of DSC or rock, collectively these complex deep reefs sustain similar ecological functions as shallow reefs, providing structure for the development of diverse benthic communities (Roberts et al., 2009; Lessard-Pilon et al.,

* Corresponding author.
E-mail address: rosss@uncw.edu (S.W. Ross).

http://dx.doi.org/10.1016/j.dsr.2016.12.005
Received 30 August 2016; Received in revised form 2 December 2016; Accepted 5 December 2016
Available online 09 December 2016
0967-0637/ © 2016 Elsevier Ltd. All rights reserved.

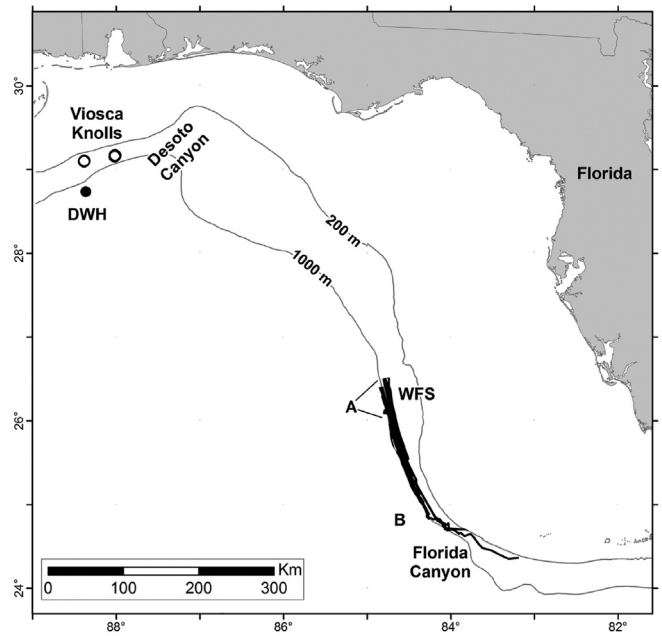

Fig. 1. North-central and eastern Gulf of Mexico illustrating locations of the two Viosca Knoll deep reef sites, the Deep-Water Horizon (DWH) well site, and the West Florida Slope (WFS) study area. Area A at the north end of the WFS study area was mapped with multibeam sonar by the NOAA ships *Nancy Foster* and *Okeanos Explorer*, was surveyed by several underwater vehicles, and is presented in greater detail in this paper. The strips (B) south of A were mapped by the M/V *Lost Coast Explorer* and the *Okeanos Explorer*.

2010). Over the last decade research programs directed toward DSC ecosystems in the GOM indicated that DSC reefs are most abundant in 300 to about 600 m depths and support distinct communities (Continental Shelf Associates, 2007; Cordes et al., 2008; Ross et al., 2012; Brooks et al., 2015).

GOM oil and gas lease blocks Viosca Knoll 826 (VK826, 415–480 m depths) and Viosca Knoll 862/906 (VK862/906, 310–440 m depths) in the north-central GOM, approximately 37 km apart (Fig. 1), were previously reported to exhibit the most extensive DSC accumulations in the GOM (Schroeder and Brooke, 2011). These sites are characterized by *L. pertusa* bioherms and carbonate blocks colonized by corals and sponges, interspersed with shell hash, coral rubble and soft sediments (Schroeder et al., 2005; Brooke and Schroeder, 2007; Continental Shelf Associates, 2007; Davies et al., 2010). Based on several years of video surveys at the VK sites, we conservatively estimated (not previously published) the areas most heavily covered by DSC (living and dead) and rocky bottom to be about 412,500 m^2 (0.413 km^2) at VK826 and about 562,500 m^2 (0.563 km^2) at VK862/906 (Supplemental Fig. 1), but note that these estimates include some non-reef, soft-bottom habitat that is not separable at this scale. A newly discovered DSC region on the Campeche Bank, dominated by *E. profunda* and L. *pertusa*, reportedly surpasses the VK region in aerial extent (4,000,000 m^2 or 40 km^2) of coral habitat (Hebbeln et al., 2014).

This paper describes extensive areas of hard substrata and DSC, some recently discovered, on the West Florida Slope (WFS) in the eastern GOM and provides the oceanographic and geological context for these sites. Associated fauna will not be described except for major sessile species which contribute to benthic habitat structure. The midpoint of this study area is about 478 and 460 km southeast of the VK deep reefs and the Deep-Water Horizon oil spill site, respectively (Fig. 1), and about 362 km northeast of the Campeche Bank deep coral mounds. Numerous small topographic highs with stands of mostly dead L. *pertusa* were described previously for part of the WFS area (Newton et al., 1987; Reed et al., 2006; Hübscher et al., 2010). Recent multibeam sonar surveys of the WFS and subsequent visual surveys revealed widespread living coral colonies capping large ridges and numerous putative DSC bioherms. The living DSC and complex habitat in this area is perhaps the most extensive in the GOM and may represent an important bridge for DSC communities between the Caribbean, the north-central GOM, and the rest of the North Atlantic. Regardless of the area's role in connectivity, the WFS is an important reservoir of upper slope biodiversity.

2. Methods

2.1. Research cruises

Six research cruises provided data for the WFS region. During 20–22 October 2008, the NOAA ship *Nancy Foster* used multibeam sonar to map areas likely to contain DSC and hard bottom habitats. Guided by these maps, the R/V *Seward Johnson* and the *Johnson Sea-Link II* submersible (JSL, Harbor Branch Oceanographic Inst., Florida Atlantic Univ.) surveyed the WFS (16–17 September 2009). The first 2010 cruise (28 September-2 October) addressed multidisciplinary research objectives using the R/V *Cape Hatteras* and the remotely operated vehicle (ROV) *Kraken II* (Univ. Connecticut). The NOAA ship *Ronald H. Brown* and ROV *Jason II* (Woods Hole Oceanographic Inst.) conducted one dive on the WFS (10 November 2010). Multibeam sonar mapping was conducted by the *Lost Coast Explorer* (7–10 November 2010). During 20–22 March 2012, the NOAA ship *Okeanos Explorer* conducted multibeam mapping and two dives with the ROV *Little Hercules* in the WFS study area. The area mapped during the 2008 cruise (Fig. 1, Area A) is emphasized because more extensive data were collected there.

2.2. Multibeam sonar surveys

Part of the WFS (Fig. 1), centered on a previously described (Newton et al., 1987; Reed et al., 2006) hardground area, was surveyed during the 2008 *Nancy Foster* cruise using a Kongsberg-Simrad EM1002 (95 kHz frequency, 111 beams per ping) multibeam sonar. An additional single track line of multibeam sonar, attempting to follow the long scarp described below, was collected south of the 2008 survey by the *Lost Coast Explorer*, using a Kongsberg EM710 (70–100 kHz frequency, 400 beams per ping) multibeam system. During the *Okeanos Explorer* cruise additional multibeam sonar data were collected using a Kongsberg EM302 (30 kHz frequency, 432 beams per ping) to fill in deeper areas not mapped in previous cruises. Raw data were corrected and post-processed using CARIS HIPS and SIPS (v. 6.1) to produce georeferenced color-shaded bathymetric maps (in ArcGIS v. 9.31, ESRI) gridded to 8 m (2008 survey), 3 m (2010 survey), and 10 and 25 m (2012 survey) resolutions.

Features of the prominent scarp were described as follows. The highest points along the top edge of the scarp were traced on the GIS map. The base of the scarp was more difficult to discern because it often exhibited slumping, multiple terraces, and boulder fields. To resolve the scarp base, the slope of each map cell (8×8 m or 10×10 m) in the raster dataset was calculated using ArcGIS, and we identified the base of the scarp as those cells where the slopes either obviously changed direction (as in boulder fields) or became flat. The scarp base was then also traced on the GIS map, and the scarp face was defined the area between the top and base lines. Vertical relief of the scarp was measured only in the 2008 survey area approximately every 50 m by subtracting the depth at the top of the scarp from that at the base. The width of the scarp was measured at the same places using the two-dimensional distance between the top and the base. The angular slopes of the scarp face were calculated at the 50 m intervals by taking the arctangent of scarp relief divided by its width.

Objectively identifying the numerous topographic highs (mounds and ridges) west of the scarp was more difficult because these features varied greatly in size and shape, were often not continuous (unlike the scarp), and geological features are frequently described in relative

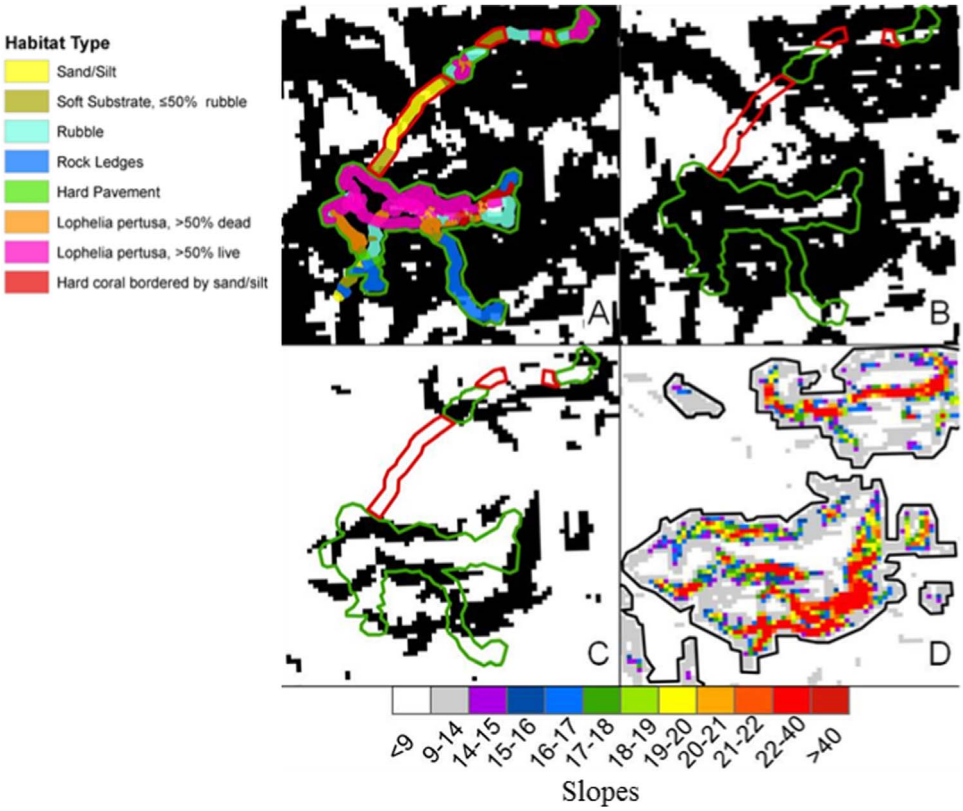

Fig. 2. Selected area of the southernmost dive sites on the WFS (see Fig. 3) illustrating sequential removal of slope cells. A portion of dive tracks is included in A with habitats color coded (see left sidebar). In B and C all reef habitats on the dive tracks are outlined in green, and non-reef habitats are outlined in red. A = black cells include all slopes ≥4°. B = black cells include slopes ≥6°. C = black cells include slopes ≥14°; note high slopes now correlated with reef areas (green outline) defined by dives. D = All slopes are color coded (bottom sidebar) and slopes ≥9° are outlined in black. In panel D five features (outlined in black) are counted as elevated reef areas. (For interpretation of the references to color in this figure legend, the reader is referred to the web version of this article.)

terms, lacking explicit criteria such as slope angles (International Hydrographic Organization, 2013). Multibeam derived topography was confirmed with visual surveys during submersible and ROV dives, which generally focused on and around the most prominent features. The areas surveyed during these dives were used to develop slope criteria to define other similar topographic highs west of the scarp. First, a slope was calculated for each map cell (8×8 m or 10×10 m) in the raster dataset using ArcGIS, and cells were color coded by slope (Fig. 2). The map was overlaid with the dive track habitat maps for this area (Fig. 2A), which were simplified to reef (green outline) versus non-reef (red outline) (Fig. 2B, C). Next, cells were sequentially removed in 1° increments (starting with 0°) until topographic features (reef or non-reef) observed during the dives were clearly defined by remaining cells. Reef features surveyed during dives were best identified when the majority of cells had slopes ≥14° (Fig. 2C); therefore, clusters of cells with ≥14° slopes were defined as mounds or ridges in the mapped area A (Figs. 1 and 3). An example of a progression of cell removal illustrates that including slope angles < 9° obscured the boundaries of large topographic features (Fig. 2A, B). To more inclusively capture areas of the mounds/ridges, all cells with a slope ≥9° were included as part of a topographic feature if they lay adjacent to the cells with slopes ≥14° (Fig. 2D).

2.3. Environmental data

Environmental data were collected throughout the water column (to within ca. 10 m of bottom) using a SeaBird SBE 911*plus* at a data logging rate of 24 samples/sec. The six CTD casts made in 2008 (Fig. 3) recorded conductivity (μS/cm), temperature (°C), depth (m, calculated from pressure), altitude (m), salinity (calculated), and dissolved oxygen (DO, ml/l) at various locations within the mapped area. Four CTD casts were made over a single coral mound (Fig. 3) in 2009, measuring the same parameters as in 2008, plus density (σ_θ, kg m^{-3}). Single CTD casts and cross-slope transects (stations spaced at ca. 500 m intervals) were completed during the 2010 R/V *Cape Hatteras* cruise (Fig. 3), measuring the same parameters as in 2009, plus pH and fluorescence (Chl-α, μg/l). For individual CTD casts, measured variables were plotted against depth. Profiles of selected variables were plotted against depth and distance along the cross-slope transects using Surfer (v. 8) software.

Environmental data were also recorded during each underwater vehicle dive. The *JSL* used a SeaBird SBE 19*plus* mounted about 2 m above its base to record conductivity (μS/cm), temperature (°C), depth (pressure), salinity (calculated), DO (ml/l), and pH once per second. The same instrument package was also attached to the ROV *Kraken II* down-weight. While the ROV was on bottom, the down weight was usually 15–20 m off bottom, but was sometimes closer to the bottom. A Seabird SBE 37-SI mounted on the ROV *Jason II* recorded conductivity (S/m), temperature (°C), and depth (pressure) once per second. Only the data recorded while the vehicles were on or near bottom are presented.

2.4. Bottom observations

High resolution video and still digital imagery were obtained during four cruises. Three dives were completed on the WFS in 2009 using the *JSL* submersible, followed by five dives in 2010 using the ROV *Kraken II*, one dive in 2010 with the ROV *Jason II*, and two dives in 2012 using the ROV *Little Hercules* (Table 1). Annotated video transects were conducted as described in Ross and Quattrini (2007).

Dive videos were viewed multiple times for habitat classifications by time of observation and to document distributions of DSC (to lowest

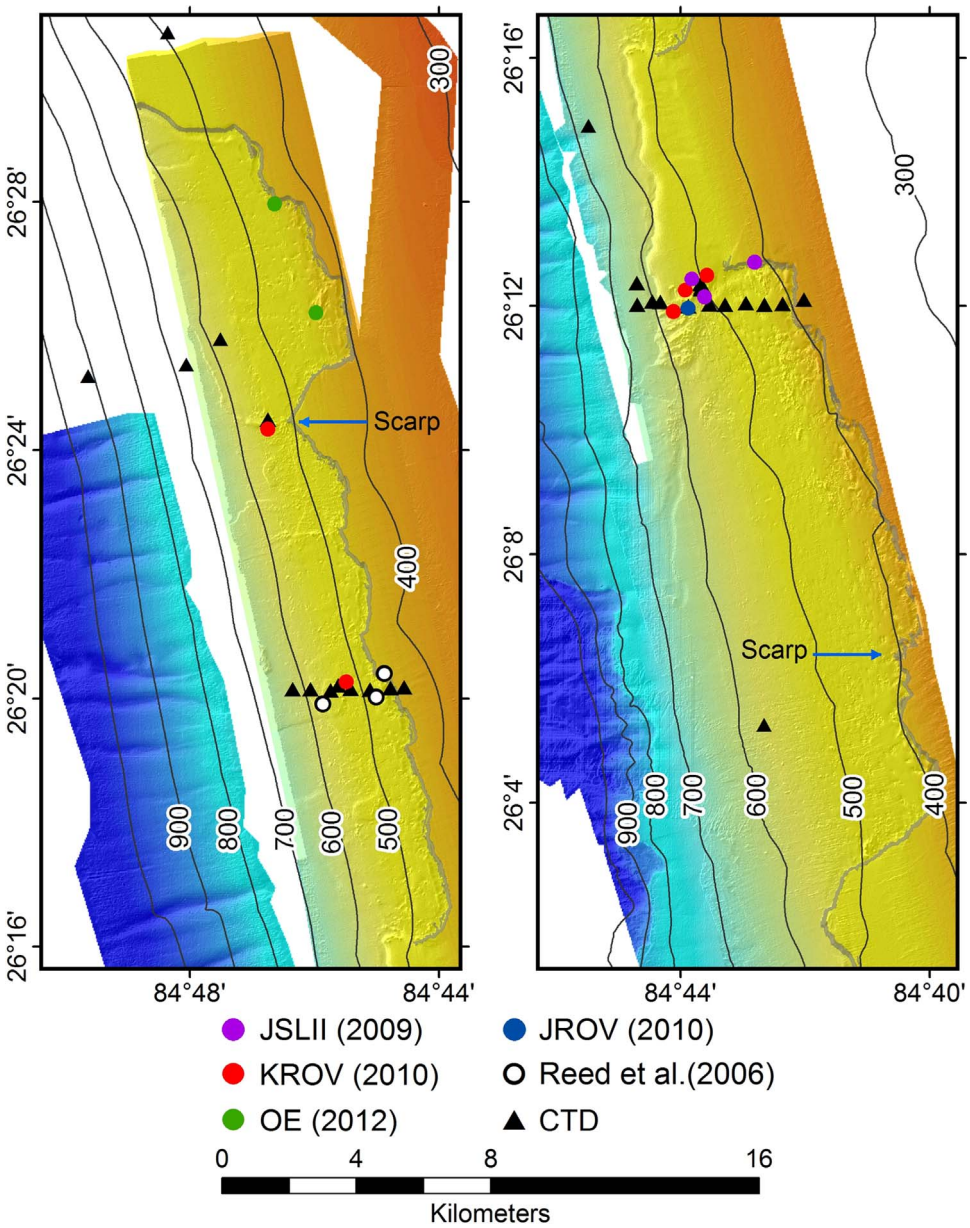

Fig. 3. Larger scale view of the West Florida Slope surveyed with multibeam sonar during the 2008 and 2012 cruises (A in Fig. 1), showing bathymetry, dive vehicle bottom starting points and CTD stations. Note the bottom of the left panel joins the top of the right panel. See Figs. 7–9 for habitat details along the dive tracks. The southernmost cluster of dives is the area also visited by Hübscher et al. (2010).

possible taxa). Benthic habitat classifications were modified from Partyka et al. (2007) and defined as follows: 1) Soft substrata (sand and/or silt), few or no hard structures; 2) Soft substrata up to 50% covered in coral rubble (small, broken, unconsolidated coral pieces, mostly *L. pertusa*) and/or small rocks, vertical height < 1 m; 3) Rubble bottom > 50% covered with coral rubble and/or small rocks, profile < 1 m; 4) Rocky ledges and/or boulders, profile > 1 m; 5) Hard pavement, profile usually flat or < 1 m; 6) Hard corals (*L. pertusa* dominated), 80–100% bottom cover, > 50% dead, profile > 1 m; 7) Hard corals (*L. pertusa* dominated), 80–100% bottom cover, > 50% live coral, profile > 1 m, usually with high % of attached sponges and other sessile fauna; 8) Isolated coral bushes surrounded by soft substrata and often a high % of surrounding coral or rock rubble. Any of the hard substrata, especially non-living components, exhibited varying amounts of attached fauna.

Submersible and ROV dive tracks were initially processed to conservatively remove erroneous tracking data (location points) as described by Quattrini et al. (2012). Location points along the track were assigned habitat codes (1–8, see above) by matching the video time of the habitat code with the track point time code. Habitats could not be assigned for some video segments (poor image quality, too far off bottom), creating a few gaps (about 10% of the total track lengths) in the otherwise continuous bottom tracks. All location points were then plotted in ArcGIS.Dive tracks were further smoothed by conducting a three point moving average of the track points using ADELIE GIS module (v. 1.8, IFREMER). Dive track lines were created using the point to line function in ADELIE with a buffer of 10 m on each side of the track line. The resulting 20 m wide dive track was used as a mask for Inverse Distance Weighted (IDW) analysis using ArcGIS.To extend habitat values along the dive track between dive track points, IDW analysis was performed (power=2 and variable radius=1) on the smoothed dive track points. Habitat coded polygons were created from the IDW rasters, and these polygons were simplified (ArcGIS), which smoothed polygon edges. To obtain relative percent habitat contributions, areas (m^2) of each habitat type were determined using the ArcGIS Geometry Calculator.

Table 1
Stations sampled on or near deep reefs in the eastern GOM during five cruises (NOAA ship *Nancy Foster* [NF], R/V *Seward Johnson* [SJ], R/V *Cape Hatteras* [CH], NOAA ship *Ronald H. Brown* [RB], NOAA ship *Okeanos Explorer* [OE]). D=Day (0700–1830 h EDT), N=Night (1830–0700 h EDT). CTD=Seabird SBE 911+, JSL=*Johnson-Sea-Link II* submersible, KROV= *Kraken II*, JROV=*Jason II*, OE ROV=*Little Hercules*. Submersible and ROV total times, latitudes, longitudes, and depth ranges are only for the period when the vehicles were on the bottom. For CTD casts, depth ranges include the maximum depth of the sample to the surface (S).

Station #	Gear	Date	Time	Total Time (min)	Start Latitude (°N)	Start Longitude (°W)	End Latitude (°N)	End Longitude (°W)	Depth Range (m)
NF-2008-084	CTD	20-Oct-08	N	18	26° 25.19	84° 49.64			S-757
NF-2008-085	CTD	21-Oct-08	N	20	26° 25.79	84° 47.51			S-562
NF-2008-086	CTD	21-Oct-08	D	21	26° 25.38	84° 48.06			S-660
NF-2008-087	CTD	21-Oct-08	D	9	26° 30.73	84° 48.36			S-449
NF-2008-088	CTD	21-Oct-08	N	13	26° 14.90	84° 45.48			S-649
NF-2008-089	CTD	22-Oct-08	D	12	26° 05.25	84° 42.66			S-553
JSLII-2009-GOM-3722	JSL	16-Sep-09	D	158	26° 12.19	84° 43.64	26° 12.31	84° 43.62	536–500
JSLII-2009-GOM-3723	JSL	16-Sep-09	D	157	26° 12.43	84° 42.73	26° 12.71	84° 42.83	428–414
JSLII-2009-GOM-3724	JSL	17-Sep-09	D	161	26° 12.23	84° 43.75	26° 12.47	84° 43.54	531–477
SJ-2009-GOM-002	CTD	16-Sep-09	N	21	26° 12.30	84° 43.66	26° 12.39	84° 43.40	S-439
SJ–2009-GOM-008	CTD	16-Sep-09	N	21	26° 12.36	84° 43.68	26° 12.34	84° 43.61	S-459
SJ-2009-GOM-012	CTD	17-Sep-09	N	15	26° 12.29	84° 43.65	26° 12.34	84° 43.58	S-437
SJ-2009-GOM-014	CTD	17-Sep-09	N	16	26° 12.27	84° 43.67	26° 12.26	84° 43.68	S-438
KROV-2010-CH-007	ROV	28-Sep-10	D	572	26° 12.51	84° 43.58	26° 12.44	84° 43.52	485–522
KROV-2010-CH-008	ROV	29-Sep-10	D	562	26° 11.75	84° 44.38	26° 11.88	84° 43.91	530–584
KROV-2010-CH-009	ROV	30-Sep-10	D	497	26° 12.26	84° 43.94	26° 12.26	84° 43.77	519–549
KROV-2010-CH-010	ROV	01-Oct-10	D	555	26° 20.15	84° 45.68	26° 20.08	84° 43.34	497–531
KROV-2010-CH-011	ROV	02-Oct-10	D	310	26° 24.46	84° 46.71	26° 24.39	84° 46.62	494–522
CH-2010-054	CTD	28-Sep-10	D	12	26° 12.35	84° 43.67	26° 12.56	84° 43.72	S-493
CH-2010-055	CTD	28-Sep-10	N	8	26° 12.10	84° 42.02	26° 12.08	84° 42.02	S-368
CH-2010-056	CTD	28-Sep-10	N	9	26° 12.03	84° 42.36	26° 12.02	84° 42.30	S-404
CH-2010-057	CTD	28-Sep-10	N	10	26° 12.02	84° 42.65	26° 12.03	84° 42.56	S-430
CH-2010-059	CTD	28-Sep-10	N	12	26° 12.02	84° 43.29	26° 12.06	84° 43.16	S-489
CH-2010-060	CTD	28-Sep-10	N	12	26° 12.03	84° 43.53	26° 12.07	84° 43.52	S-519
CH-2010-059	CTD	28-Sep-10	N	12	26° 12.02	84° 43.29	26° 12.06	84° 43.16	S-489
CH-2010-061	CTD	28-Sep-10	N	13	26° 11.99	84° 43.88	26° 12.09	84° 43.76	S-527
CH-2010-062	CTD	29-Sep-10	N	14	26° 12.06	84° 44.33	26° 12.14	84° 44.43	S-600
CH-2010-063[a]	CTD	29-Sep-10	N	11	26° 12.07	84° 44.46	26° 12.06	84° 44.51	S-602
CH-2010-064	CTD	29-Sep-10	N	12	26° 12.02	84° 44.70	26° 12.11	84° 44.74	S-632
CH-2010-074	CTD	29-Sep-10	N	18	26° 12.37	84° 44.71	26° 12.63	84° 44.03	S-647
CH-2010-085	CTD	01-Oct-10	N	10	26° 20.20	84° 45.62	26° 20.21	84° 45.56	S-509
CH-2010-086	CTD	01-Oct-10	N	8	26° 20.17	84° 44.56	26° 20.19	84° 44.52	S-389
CH-2010-087	CTD	01-Oct-10	N	9	26° 20.16	84° 44.77	26° 20.17	84° 44.80	S-453
CH-2010-088	CTD	01-Oct-10	N	10	26° 20.14	84° 45.10	26° 20.15	84° 45.10	S-465
CH-2010-089	CTD	01-Oct-10	N	11	26° 20.15	84° 45.41	26° 20.16	84° 45.39	S-478
CH-2010-090	CTD	01-Oct-10	N	12	26° 20.12	84° 45.74	26° 20.15	84° 45.70	S-507
CH-2010-091	CTD	01-Oct-10	N	15	26° 20.14	84° 46.06	26° 20.17	84° 45.99	S-550
CH-2010-092	CTD	01-Oct-10	N	14	26° 20.14	84° 46.35	26° 20.16	84° 46.29	S-588
CH-2010-098	CTD	02-Oct-10	N	10	26° 24.49	84° 46.74	26° 24.51	84° 46.69	S-498
JROV-2010-RB-542	ROV	10-Nov-10	N	320	26° 11.92	84° 44.05	26° 12.29	84° 43.71	492–555
OE-ROV-01	ROV	20-Mar-12	D	367	26° 28.00	84° 46.71	26° 28.77	84° 46.37	395–452
OE-ROV-02	ROV	22-Mar-12	D	403	26° 26.21	84° 45.81	26° 26.29	84° 45.89	396–429

[a] Data logger malfunctioned; data not used.

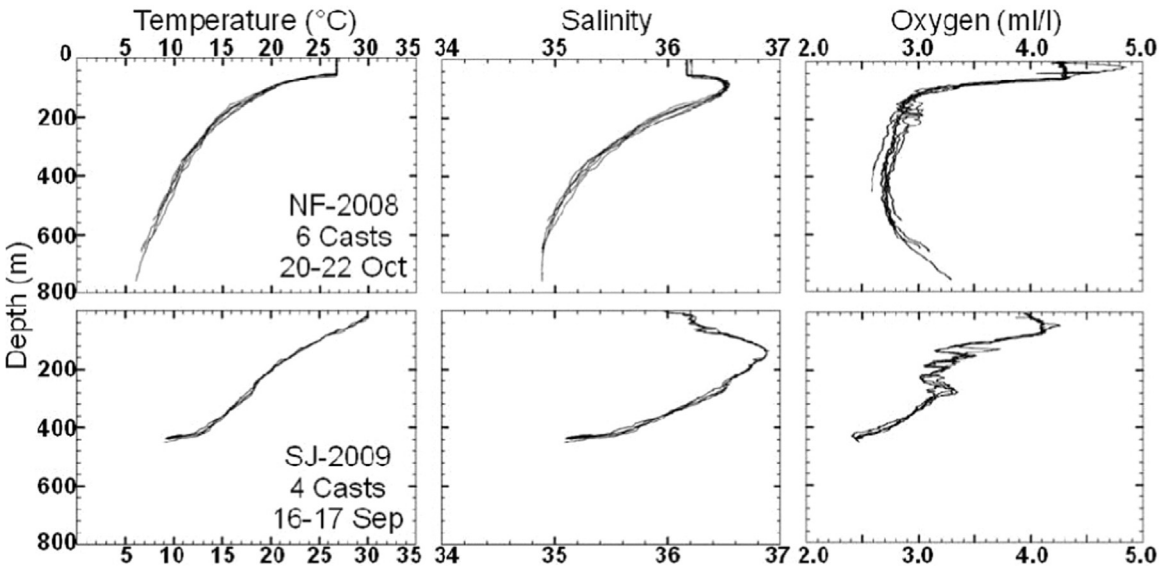

Fig. 4. Temperature, salinity, and dissolved oxygen plots versus depth. The upper panel six CTD casts conducted during the *Nancy Foster* cruise (20–22 October 2008) occurred throughout the area of multibeam sampling, and the lower panel data of the four casts from the *Seward Johnson* cruise (16–17 September 2009) were all collected over the same coral mound (see Fig. 3 and Table 1 for locations).

3. Results

3.1. Water mass characteristics

Thirty-one water column CTD casts were made during three cruises (Table 1). Although the six casts made during the October 2008 cruise covered a large area (Fig. 3) spread over three days, data were comparable among casts, and all casts were plotted together (Fig. 4, upper panels). A sharp thermocline was observed between 50–60 m, with temperature declining rapidly from about 27 °C to 15–16 °C at a depth of about 200 m and thereafter declining less rapidly to about 6 °C at 757 m. Salinity exhibited a maximum (~ 36.5) between 60–100 m and steadily declined toward 35 with increasing depth. Except for station NF-2008-084, which exhibited unusually high (almost 5.0 ml/l) DO in the surface waters, all other DO data from these casts exhibited a sharp decline at the thermocline, reaching an oxygen minimum (2.7–2.8 ml/l) around 200 m. The oxygen minimum layer persisted to about 600 m, with oxygen values rising (to 2.8–3.5 ml/l) with increasing depth thereafter.

The four CTD casts made during 16–17 September 2009 over the same coral covered mound (Fig. 3, Table 1) exhibited little variation, so these data were plotted together (Fig. 4, lower panels). Unlike the other CTD casts, these profiles exhibited warmer (30 °C) surface temperatures, and temperatures started to decline at a relatively shallow depth with no clear thermocline, until about 400 m where temperature dropped rapidly toward 10 °C with increasing depth. Temperatures were warmer at all depths compared with data from the other cruises. Salinity overall and the salinity maximum (ca. 36.8) were also higher for these four casts compared with the other salinity data. DO values declined with depth (except for higher levels in the 40–60 m depth band), but also exhibited variability with depth and no clear oxygen minimum layer. DO reached lower values (2.4 ml/l at 459 m) at this site than those observed at most other sites or times (Figs. 4 and 5).

The two cross-slope CTD transects conducted during the 2010 *Cape Hatteras* cruise (Fig. 5) exhibited similar water mass patterns. There was little variability in parameter values across the transect stations at the same depths; most differences occurred with changing depth. Obvious changes in most parameters occurred between about 50 and 100 m depths. As in the water column casts described above, both transects revealed a high salinity (36.7) signature near 100 m that persisted across the transects, and with increasing depth salinity declined slowly toward 35 at the deepest stations. DO patterns were similar in both transects, except that high oxygen values (ca. 4 ml/l) persisted from the surface to a greater depth in the northern transect compared to the southern transect. A DO minimum (ca. 2.6 ml/l) layer, nearly 200 m thick, occurred in the depth zone occupied by DSC. Cross-slope near bottom temperatures were 9.7 and 11.0 °C at 390 and 369 m (stations 086 and 055, respectively) and dropped to 7.0 and 6.9 °C at 589 and 634 m (stations 092 and 064, respectively) (Fig. 5). Near-bottom temperatures in the vicinity of coral habitats on the north transect were 7.6–8.3 °C (535–500 m). For the southern cross slope transect, near-bottom temperatures above the shallower coral habitat were 9.5–9.9 °C at 410–425 m, and above the deeper coral habitat near bottom temperatures were 7.0–8.8 °C at 505–620 m. Chlorophyll-α activity estimated by fluorescence exhibited typical patterns (higher concentrations near-surface, declining with depth) in both cross-slope transects (Fig. 5). But, in the northern transect (1 October 2010) a narrow more intense band of fluorescence was centered around 100 m compared with a more diffuse, thicker band in the upper 100 m of the southern transect (28–29 September). Other water column data did not reflect those fluorescence patterns (Fig. 5).

Bottom-water characteristics relevant to benthic habitats were recorded during the submersible and ROV dives. During the two JSL dives on the ridges west of the scarp (JSLII-2009-GOM-3722, 3724) bottom temperature, salinity and DO varied little during the time on bottom (Table 2) despite the JSL covering depth ranges of 36 and 54 m, respectively, and substantial horizontal distances (100 s of meters) (Table 1). Also, little variability was observed for these parameters during a JSL dive (JSLII-2009-GOM-3723) on the rocky scarp, except when bottom temperature varied erratically over a range of nearly 2 °C in the last hour of the dive. Salinity exhibited minor variations during this period, and no obvious water mass anomalies or abrupt changes in depth were observed. The highest bottom water temperature (10.2 °C) was recorded during this scarp dive, which was also the shallowest dive that recorded temperature data (Table 1). Near-bottom environmental data recorded during *Kraken* dives exhibited some variability (Table 2) due to vertical movement of the down weight (location of sensors) in the water column. Usually the variations in temperature, salinity and DO were small during the five *Kraken* dives and were similar to those recorded during the other dives (Table 2). Dive KROV-2010-CH-008 and to a lesser extent dive 010 exhibited the highest variability in near bottom water temperature, DO

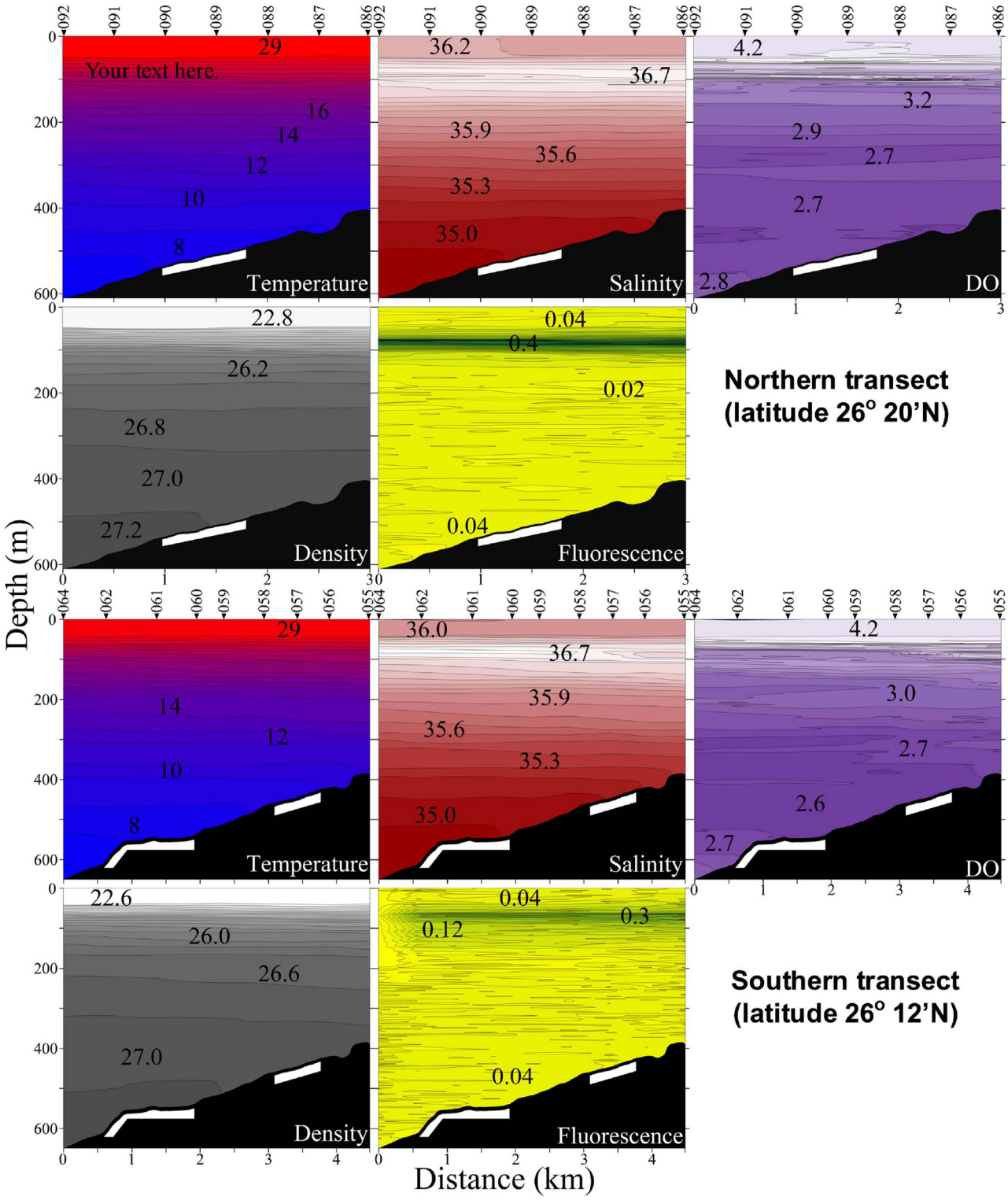

Fig. 5. Cross-slope transects of temperature (° C), salinity, dissolved oxygen (DO, ml/l), density (σ_θ, kg m^{-3}) and fluorescence (Chl-α, μg/l). The northern transect (upper panels) was conducted on 1 October 2010 and the southern transect (lower panels) on 28–29 September 2010 (see Table 1 for station details). The distance scale originates at the offshore stations with stations at approximately 500 m intervals (See Fig. 3). The white bars represent the approximate locations of coral covered mounds near the transects. Bathymetry was derived from the 2008 multibeam sonar survey.

and salinity, but these variations probably resulted from rough seas and strong currents that caused the down-weight to move through a larger than usual part of the water column. When the weight was pulled upward, temperatures increased and were accompanied by a decrease in DO. DO < 1.8 ml/l was recorded for almost two hours during dive 008, and this very low DO water overlying the coral covered ridge was the lowest recorded during the study. The *Jason* dive covered a vertical depth range of 63 m on bottom (Table 1) and recorded similar bottom-water temperatures (mean=8.5 °C) and nearly the same salinity patterns compared with other dives (Table 2).

During the six cruises, the main body of the Loop Current (LC) was far south or west of the WFS study sites (Fig. 6). A south-flowing

Table 2
Bottom or near-bottom environmental data recorded during *Johnson-Sea-Link II* (JSLII), *Kraken II* (KROV), *Jason II* (JROV) dives on the West Florida slope deep-sea reefs. Data are means ± SE of the means with ranges in parentheses during the bottom time portion of the dives. DO=dissolved oxygen. See Table 1 for dive dates, bottom time durations and depth ranges.

Dive	Temperature (°C)	Salinity	DO (ml/l)
JSLII-2009-GOM-3722	8.1 ± 0.0 (8.0–8.2)	35.0 ± 0.0 (34.9–35.0)	2.7 ± 0.0 (2.6–2.8)
JSLII-2009-GOM-3723	8.4 ± 0.2 (8.3–10.2)	35.0 ± 0.0 (34.8–35.4)	2.7 ± 0.0 (2.6–2.8)
JSLII-2009-GOM-3724	7.9 ± 0.0 (7.9–8.0)	35.0 ± 0.0 (34.9–35.0)	2.7 ± 0.0 (2.7–2.8)
KROV-2010-CH-007	8.5 ± 0.3 (8.1–9.1)	35.0 ± 0.0 (35.0–35.1)	2.7 ± 0.0 (2.7–2.8)
KROV-2010-CH-008	8.2 ± 0.3 (7.7–9.8)	34.3 ± 0.4 (33.2–35.0)	2.2 ± 0.4 (1.4–2.8)
KROV-2010-CH-009	8.3 ± 0.1 (8.1–8.6)	35.0 ± 0.0 (34.8–35.1)	2.7 ± 0.0 (2.7–2.7)
KROV-2010-CH-010	8.1 ± 0.4 (7.8–8.5)	35.0 ± 0.0 (34.8–35.0)	2.6 ± 0.1 (2.5–2.8)
KROV-2010-CH-011	8.4 ± 0.0 (8.2–8.6)	35.0 ± 0.0 (34.9–35.0)	2.7 ± 0.0 (2.6–2.7)
JROV-2010-RB-542	8.5 ± 0.2 (8.0–8.6)	35.0 ± 0.0 (34.9–35.1)	

surface current would be expected if the eastern arm of the LC were present, but surface currents in the study area were often setting to the northwest during the cruises. In October 2008 the WFS study area was between the LC and a cold-core cyclonic eddy. A trailing remnant of the main LC was near the area in September 2009 and may have influenced the different water profile patterns recorded during the 2009 cruise (Fig. 4, lower panel). LC patterns in September and November 2010 were similar to each other with minimal penetration of the LC into the GOM. During those months a large cold-core eddy was north of the LC and was either south of (September) or over (November) the main WFS study area. The greatest penetration of the LC into the GOM was observed during the March 2012 cruise; however, the LC remained well west of the study area (Fig. 6).

3.2. Benthic terrain

An area of the WFS extending over a distance of about 323 km and covering a total area of about 2479 km^2 (Fig. 1) was mapped with multibeam sonar. The most prominent feature in the multibeam maps is a north-south trending scarp, the top of which usually occurs at depths of 375–500 m (average depth at top of scarp =440 m) and which is recognizable almost continuously for about 88 km (from ~ 26° 29.5′ N to ~ 25° 52.3′ N). South of 25° 52.3′ N the scarp was not always obvious from the multibeam data but could still be traced for an additional 141 km, yielding a total length of about 229 km. The area of the scarp face in the region of the 2008 survey (Fig. 3) encompassed about 9.8 km^2, and its width (horizontal distance between top and base) ranged from 103 to 680 m (mean=241 m). This portion of the scarp exhibited vertical heights of about 7–85 m, with an average height of 47.5 m (±13.3 SD). Angular slopes across the scarp face ranged from 1.5 to 20.4°, with some small scale local slopes estimated from submersible or ROV observations to be as steep as 90°. This part of the scarp exhibited numerous indentations and some changes in direction as abrupt as 90° (Fig. 3). Although not completely mapped, the southern continuation of this scarp had vertical heights that ranged from 20 m in the northern part increasing to as much as 200 m in the south (around 24° 37′ N).

Numerous scattered mounds and ridges occur west of the scarp. In the area in Fig. 3 and to a lesser extent south of this area to at least 25° 15′ N, some mounds and ridges occur immediately adjacent to the rocky scarp and others range up to 4200 m west of the scarp. In the mapped area of Fig. 3 between about 400 and 700 m depths, we counted 907 discrete mounds and ridges with slopes ≥14°, covering in total about 14 km^2 (area includes parts with slopes ≥9°, see methods). Vertical relief of these features was 6–37 m (mean =15.2 m, SD =5.84, n=91) (Figs. 7–9). Most of these hardbottom features occurred in depths between 450–550 m and were relatively uncommon below 600 m. Unlike the scarp (Fig. 7), large areas of dead and living DSC colonies (dominated by *L. pertusa*) occurred on nearly every mound or ridge where visual observations were recorded (Figs. 8 and 9). On the sites where we made bottom observations (Figs. 8 and 9), the area of reef habitat west of the scarp was estimated to be about 1,726,650 m^2 (1.73 km^2) (S1 Fig., right panel inside black boxes). This area included DSC, rocky structures, and some non-reef (soft substrata) habitat. Relatively small areas of non-reef sandy bottom were included because they were inseparable from reef areas on the scale (10 s of meters) of our mapping.

3.3. Benthic habitat characterization

Three submersible dives and eight ROV dives on the WFS resulted in 67.7 h of bottom observations over a total combined vehicle track distance of 56,746 m (56.75 km) (Table 1). The north-south trending scarp (observations from dives JSLII-2009-GOM-3723, OE-ROV-01, OE-ROV-02) was composed entirely of large rocky ledges and boulders with varying densities of attached, sessile invertebrates, including scattered small colonies of *L. pertusa* (Fig. 10A), and associated mobile fauna (Figs. 7 and 10A, B). In the vicinity of the JSL dive, the scarp exhibited a 90° turn to run east-west before turning back north-south (Figs. 3 and 7). These scarp ledges were less heavily populated with fauna than the features to the west.

The mounds and ridges west of the scarp comprised a mix of various sized rocks and *L. pertusa* bioherm structures, usually with coarse, sandy sediments between topographic highs (Figs. 8 and 9). In places the rocky ledges and boulders were similar in appearance to the scarp, with rocks varying in color from white to shades of grey to black (Fig. 10C). Large rocks were most commonly observed at the bases and along the lower slopes of most of the ridges. Coral cover (both dead and living *L. pertusa* colonies, Fig. 10D, E) increased toward the crests of ridges and mounds, where the substratum was a mixture of fine sediments trapped in coral rubble. These structures appeared to be *L. pertusa* bioherms on top of a basement layer of rocks. Living coral colonies were most abundant on the highest parts of mounds; however, observed live coral density was not higher on any particular side of the mounds. More dead coral occurred on mounds below a depth of about 525 m compared with shallower depths (Figs. 8 and 9).

Habitats observed along the dive tracks were dominated by various types of hard-bottom complex structure (habitat types 3–8) (Table 3). Since visual surveys targeted elevated features, these observations under-represent non-reef benthic habitats on the WFS. The most common structure-forming habitat type was high profile, mostly living *L. pertusa* (32.42% of area surveyed), followed by high profile, mostly dead *L. pertusa* (19.20%), rocky ledges or boulders (17.48%) and rubble (14.28%). Low profile, hard pavement (0.35%) was the least common hard substratum (Table 3). In addition to *L. pertusa*, other colonial scleractinians included *Madrepora oculata*, which commonly occurred in close association with *L. pertusa* (but not observed on the scarp) and *Enallopsammia profunda*, which was relatively rare (especially as living colonies). The cup coral *Thecopsammia socialis* often densely colonized dead *L. pertusa* and was also attached to exposed rocks on the scarp and elsewhere. Antipatharian corals (particularly red and white morphotypes of *Leiopathes* sp.) were

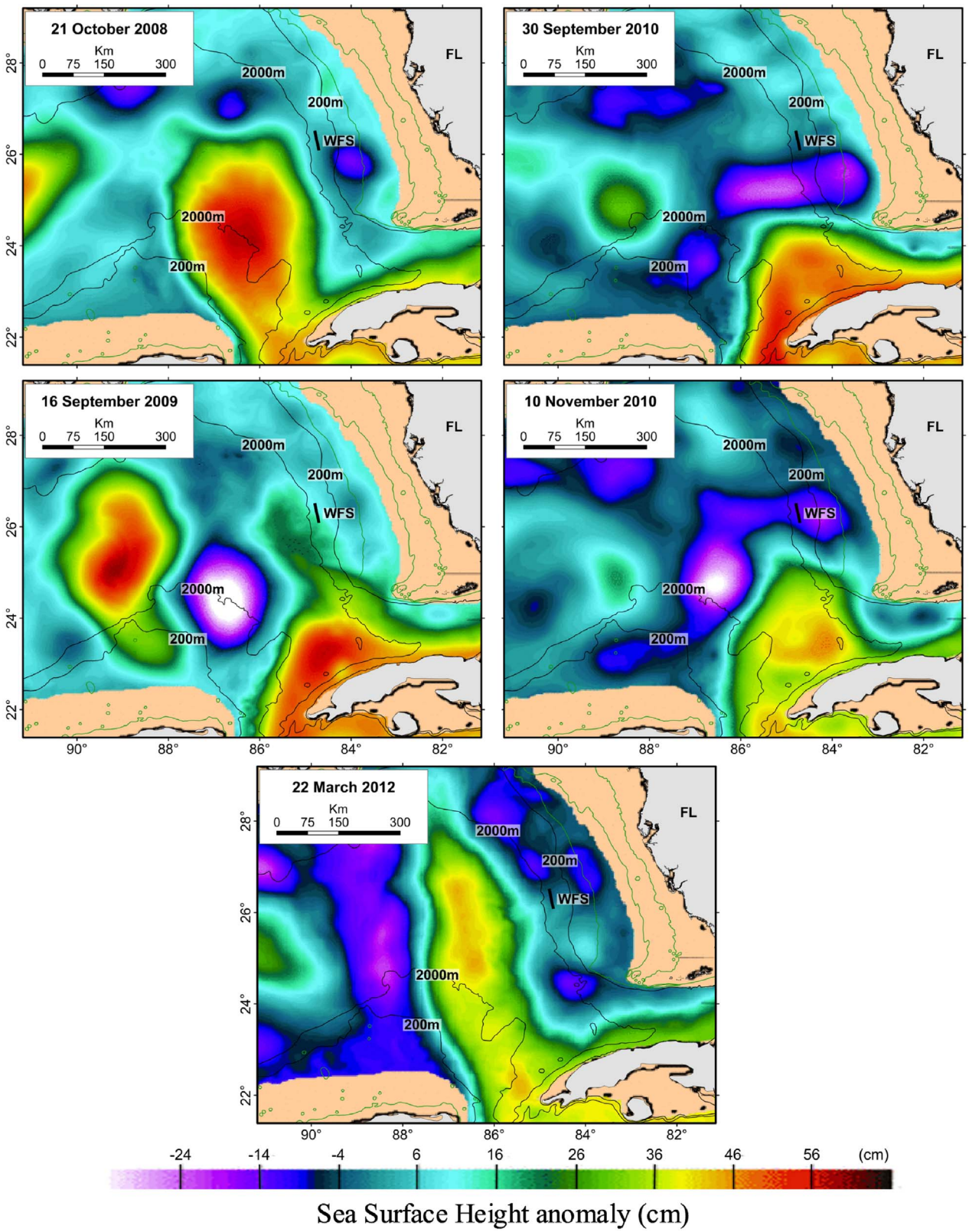

Fig. 6. Naval Research Lab Layered Ocean Model (high resolution) assimilating Sea Surface Height (SSH) for five dates during this study's cruises. The anomaly SSH satellite maps show the difference in measured sea height from the calculated mean sea level. A +17 cm SSH contour generally tracks the Loop Current and LC rings. Reds and yellows indicate higher SSH and warmer waters of the LC and LC eddies. Blue to purple colors are negative SSH anomalies, representing cold-core cyclonic eddies. The black rectangle is the main WFS study area (A in Fig. 1). (For interpretation of the references to color in this figure legend, the reader is referred to the web version of this article.)

usually restricted to the rocky structures (Fig. 10C) rather than *L. pertusa* dominated areas. Nephtheid octocorals (soft corals) occurred most commonly on the L. *pertusa* rubble zones but were also attached to rocks. Two other octocorals, *Anthomastus* sp. and *Plumarella dichotoma*, were common in coral rubble zones and attached to intact living and dead *L. pertusa*. The hydrocoral *Stylaster erubescens* and

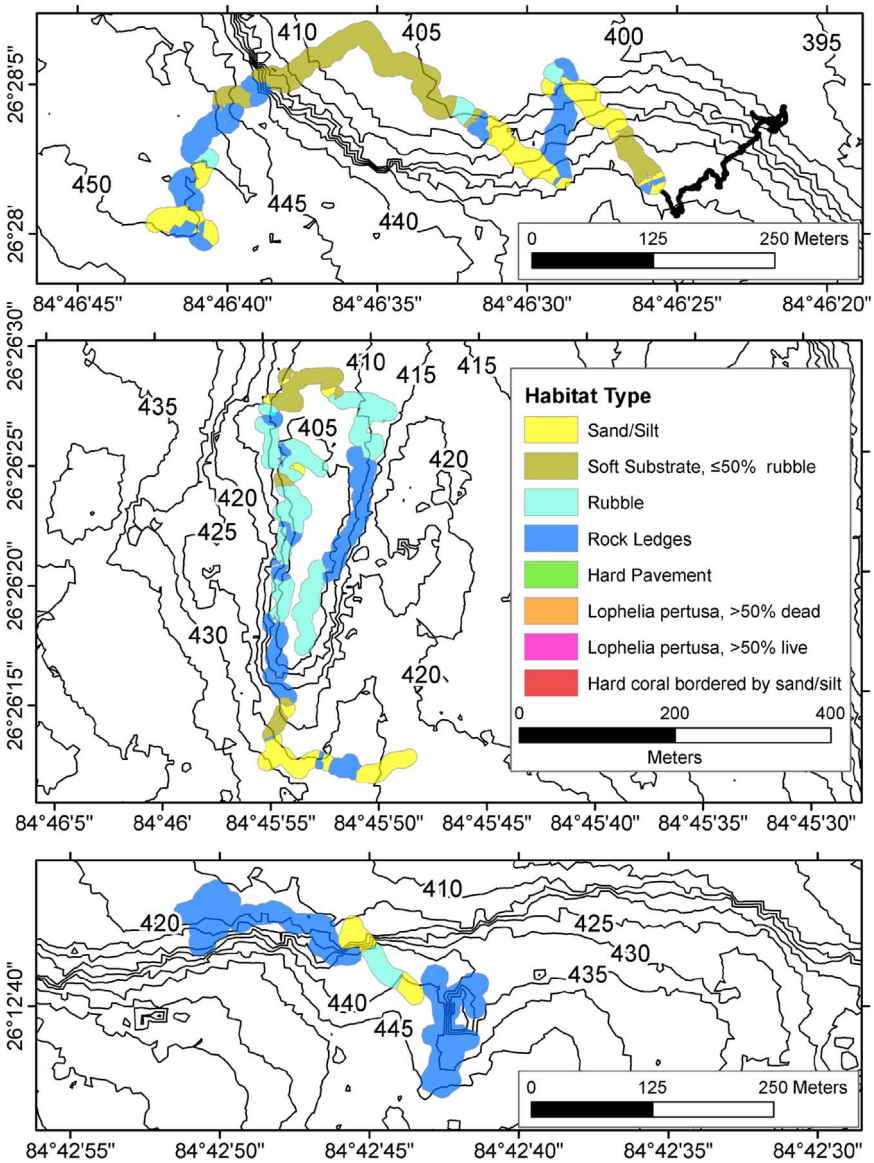

Fig. 7. WFS dive track habitat maps along the rocky scarp, north to south. Upper panel is dive OE-ROV-01, middle panel is OE-ROV-02, bottom panel is JSL3723 (see Table 1). The black track line on the eastern end of the OE-ROV-01 dive shows the ROV track, but there were no video data.

other stylasterid species were commonly attached to both rocky structures and dead *L. pertusa*.

Lost commercial fishing gear and trash were observed on a few occasions, but they were not pervasive. These included pieces of monofilament tangled in the corals and traps (~1×1 m) that were snagged in the rocks or corals. Some traps had buoy lines, one of which supported small colonies of *L. pertusa*.

4. Discussion

4.1. Oceanography

Several water masses are evident in the WFS study area. As at the Viosca Knoll coral mounds (Davies et al., 2010; Ross et al., 2010; Mienis et al., 2012), the upper 200 m of the WFS water column contained the high salinity signature of Subtropical Underwater (SUW) (Paluszkiewicz et al., 1983; Jochens and DiMarco, 2008; this study). Maintenance of high salinities (> 36.5) in this layer reflects lack of mixing and/or proximity to the Loop Current or a LC eddy (Jochens and DiMarco, 2008). The upper portion of Antarctic Intermediate Water (AAIW), characterized by lower salinity (35) than the SUW (Jochens and DiMarco, 2008) was identified in our deeper (> 500 m) CTD data. Under certain conditions this cold, nutrient-rich water is upwelled into shallower depths, as observed by intrusion of clearer, colder AAIW water at VK826 (Mienis et al., 2012) and also observed along the eastern Campeche Bank (Hebbeln et al., 2014). The low oxygen layer present throughout the WFS in the 400–500 m depth range (approximate depth of most living DSCs) is indicative of the North Atlantic Central Water. DSC in the GOM appear to generally occupy areas of low (< 3.0 ml/l) DO (Davies et al., 2010; Ross et al., 2010; Lunden et al., 2014), which could impair growth rates or increase mortality (Davies et al., 2010; Lunden et al., 2014). However, extensive, living colonies of *L. pertusa* often occur where low DO conditions are common (Campeche Bank, WFS, Viosca Knolls, North Carolina), and this coral appears to be highly tolerant of low DO concentrations (Dodds et al., 2007; Brooke et al., 2009; Hebbeln et al., 2014). Even so, Lunden et al. (2014) reported complete mortality of *L. pertusa* under prolonged exposure to DO around 1.57 ml/l, but suggested that GOM populations of this coral may be more adapted to low DO conditions than elsewhere in the Atlantic.

Interactions of the Loop Current and associated rings with the WFS and adjacent shelf are similar to Gulf Stream boundary current

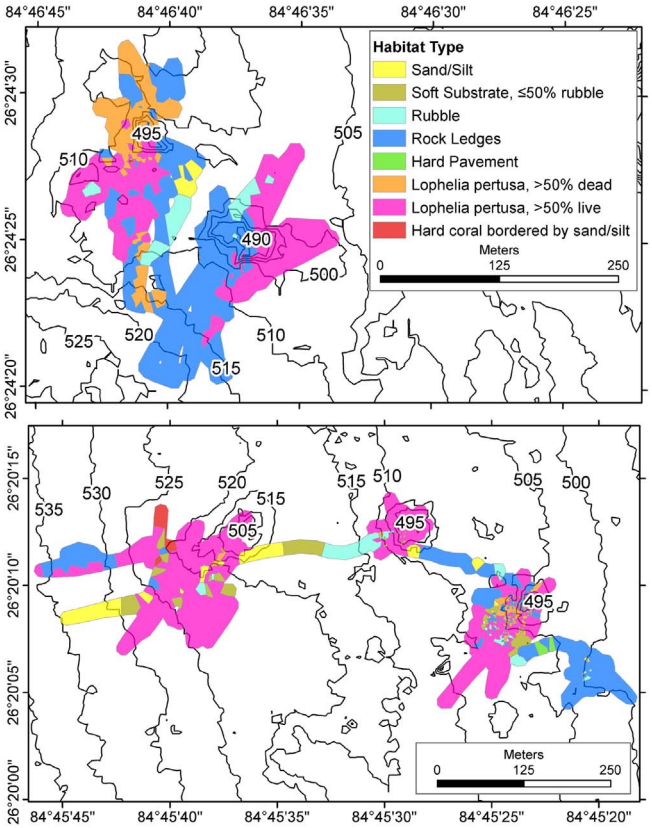

Fig. 8. WFS dive track habitat maps of the mounds/ridges west of the rocky scarp. Upper panel is dive KROV011, bottom panel is KROV010 (see Table 1).

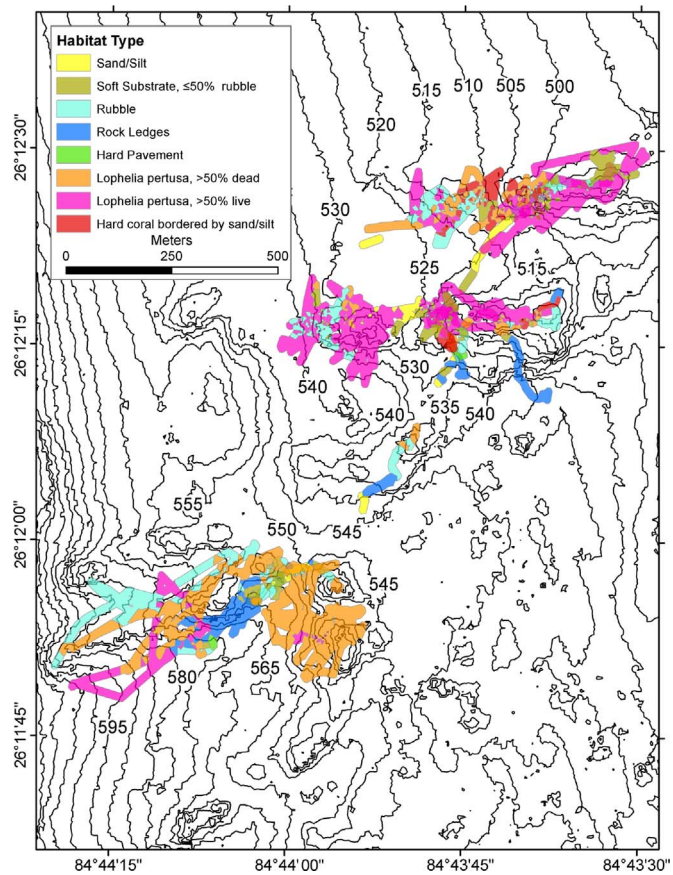

Fig. 9. WFS dive track habitat maps of the mounds/ridges west of the rocky scarp. The southern tracks are from dives JROV542 and KROV008; middle tracks are from JSL3722 and 3724 and KROV009; northern tracks are from JSL3724 and KROV007 (see Table 1).

interactions along the Atlantic slope off the SE United States (Paluszkiewicz et al., 1983; Vukovich and Maul, 1985) with eddies, meanders, upwelling, and diverse current patterns influencing climate, oceanography and biology. As observed during this study, the LC presently may have only limited direct contact with the DSC depth zone on the WFS, but it may have been more active in eroding the WFS during past lower sea levels (Doyle and Holmes, 1985). The LC meanders laterally and its variable degree of penetration into the GOM is controlled by its position and flow through the Yucatan Channel (Molinari and Morrison, 1988; Candela et al., 2002). On average, the LC reaches maximum northward intrusions in winter (in contrast to Hübscher et al., 2010) or early summer (Behringer et al., 1977; Molinari, 1980; Maul and Vukovich, 1993). During our cruises, the LC was usually south of the main study area, as is common in the fall, and the similarity of water column patterns over three years suggests longer term consistency in these conditions (at least in the fall). Even when the LC strongly penetrates the GOM, the south flowing eastern limb is often west of the WFS deep-reef sites. Deeper bottom currents under the LC off the WFS often flow northward or north-westward (Hamilton, 1990), and northward flows of deep water along the margins of the LC occur periodically (Molinari and Mayer, 1982; Vukovich and Maul, 1985). Hübscher et al. (2010) suggested that north-flowing bottom currents caused much of the erosion along the WFS scarp, although this was not based on oceanographic measurements. Lindberg and Lockhart (1993) also reported a north-flowing bottom current in this area.

Current patterns likely play important roles in slope-depth faunal connectivity between the GOM and the western North Atlantic. For example, *L. pertusa* spawns in the fall in the GOM (Brooke, in press), and since the LC often exhibits limited penetration into the GOM in the fall or is westward of the WFS, transport of *L. pertusa* larvae by the LC from the WFS into the Atlantic may be restricted. Instead, the frequent north-flowing bottom currents noted above could send WFS larvae further into the GOM. Such potential limits to dispersal during the spawning season may explain the genetic separation between populations of *L. pertusa* from the north-central GOM and those in other parts of the North Atlantic (Morrison et al., 2011). Similarly, lack of LC penetration into the GOM and interference from LC rings prevented most of the oil from the Deep-Water Horizon oil spill from entering the Atlantic or affecting the west and east Florida coasts (Liu et al., 2011). Young et al. (2012) noted that planktonic larval duration was strongly correlated with maximum dispersal distance and predicted that several deep-sea species exhibiting larval durations ≥210 days should be able to disperse considerable distances along the US east coast from the north-central GOM. However, larvae with shorter lifespans would be retained closer to the region where spawned. Laboratory studies suggest a larval duration of 20–56 days for L. *pertusa* (Larsson et al., 2014), with the shorter duration more likely *in situ*. This relatively short larval duration suggest regional, rather than basin-scale dispersal potential for L. *pertusa*. Thus, currents, reproductive timing, and larval duration may often limit GOM L. *pertusa* to relatively localized recruitment within the GOM. Given current patterns and biology noted above, L. *pertusa* from the WFS are likely more closely related to conspecifics in the northern GOM than elsewhere in the North Atlantic (an hypothesis that requires testing), but deviations from the average oceanographic conditions may facilitate periodic transport of larvae into the Atlantic, thereby maintaining some level of gene flow as reported by Morrison et al. (2011). The wider occurring lineage of the black coral, *Leiopathes* cf. *glaberrima*, exhibited a homogeneous population structure across the GOM (including WFS and VK sites, Brooks et al., 2016), but Atlantic relationships remain unknown. In

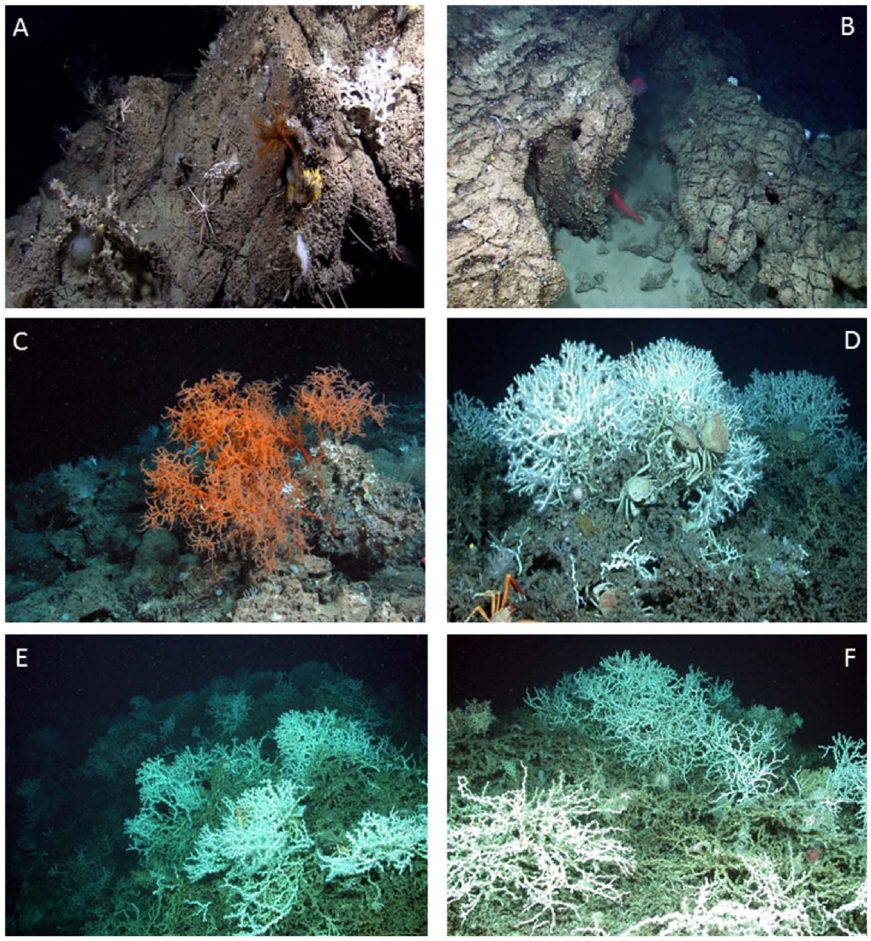

Fig. 10. Images of WFS bottom habitats. A: WFS rocky scarp illustrating bare rock as well as associated fauna (e.g., *Lophelia pertusa* in upper right corner, red comatulid crinoid in right center, the echinoid *Cidaris* sp. in center, white hexactinellid sponge in left foreground), B: View of the rocky scarp illustrating more barren area, C: Rocky ridge west of the scarp with attached large red antipatharian (*Leiopathes* sp.), D: Golden crabs, *Chaceon fenneri* (center), closely associated with living and dead *L. pertusa* on top of a mound, D-F: Dense living *L. pertusa* on the top of mounds west of the scarp.

contrast, WFS octocoral communities may differ genetically from those of the north-central GOM because of a biogeographic boundary at mid-slope depths, perhaps caused by a LC barrier (Quattrini et al., 2014), but the influences of reproductive timing, larval biology, and response to currents for these octocorals are not known. To better understand the recruitment and distribution dynamics of L. *pertusa*, genetic relationships between populations within the GOM and those upstream (e.g., on the Campeche Bank) and downstream (off the SEUS) need to be clarified.

Most well-developed DSC stands along continental margins are associated with areas of high nutrient input to surface waters from upwelling or freshwater flow, resulting in enhanced productivity and particle delivery to the seafloor (Roberts et al., 2009). The increased surface primary productivity resulting from the influx of nutrient-rich, Mississippi River derived waters may ultimately support the dense coral communities at the Viosca Knolls (Mienis et al., 2012). Primary productivity on the WFS is also enhanced by upwelling of colder, nutrient-rich waters as a result of fluctuations in the LC (Paluszkiewicz et al., 1983; Vukovich and Maul, 1985; He and Weisberg, 2003). Compared with the outer shelf, higher bottom organic carbon values were reported on the upper slope near the deep reefs described here, and this could result from increased primary productivity associated with the LC (Mullins et al., 1988a). Newly discovered DSC communities off northeastern FL (Ross et al., 2015) as well as the extensive DSC

Table 3
Habitat types (m^2) calculated over the dive tracks of JSL and ROV dives on the West Florida slope. 1=sand/silt; 2=soft substrate, $\leq$50% rubble; 3=rubble; 4=rock ledges; 5=hard pavement; 6=*L. pertusa*, >50% dead; 7=*L. pertusa*, >50% live; 8=hard coral bordered by sand/silt. Dives 007-011are *Kraken II* ROV, 3722–3724 are *JSLII*, 542 is the *Jason II* ROV, and 01–02 are *Little Hercules* ROV. See Table 1 for dive station details and see Methods for habitat definitions.

Habitat	007	008	009	010	011	Dives 3722	3723	3724	542	01	02	Totals	%
1	1233	328	2113	3899	646	0	1377	2990	2421	5630	4980	25,617	5.66
2	6697	3215	5296	3561	0	414	0	2964	2296	7448	4141	36,032	7.96
3	8065	19419	5759	2718	2145	2014	869	2395	6327	943	14006	64,660	14.28
4	9	10244	0	12894	18546	4886	11407	1400	3314	6517	9938	79,155	17.48
5	0	582	0	350	0	0	0	261	370	0	0	1,563	0.35
6	11879	60437	1560	1182	5758	1681	0	1895	2574	0	0	86,966	19.20
7	32070	15170	33386	33074	14817	11356	0	5098	1844	0	0	146,815	32.42
8	8240	65	1413	937	0	1435	0	0	0	0	0	12,090	2.67
Totals	68193	109460	49527	58615	41912	21786	13653	17003	19146	20538	33065	452,898	

province recently described on the northeastern Campeche Bank (Hebbeln et al., 2014) also occur in areas of high surface productivity driven in part by upwelling.

4.2. Geological Structure

Deep reefs occur within at least two quite different geological provinces along the GOM continental slope (Bouma and Roberts, 1990; Roberts, 2011). The north-central GOM is a siliciclastic province with numerous salt diapirs, hydrocarbon seeps, and hard substrata produced by authigenic carbonate precipitation. In contrast, the WFS, (De Soto Canyon to the Straits of Florida), is a complex, relatively smooth, carbonate ramp transition zone between the continental shelf and the GOM basin (Doyle and Holmes, 1985; Mullins et al., 1988a, 1988b). The narrower southern subsection of the WFS containing our study area exhibits steeper slopes and more frequent hardbottom outcroppings than the northern subsection (Brooks and Holmes, 2011). The 400–600 m depth zone is characterized by outcrops of phosphorites and carbonate hardgrounds surrounded by coarse grained, winnowed sediments (Mullins et al., 1988a); however, outcrops are rare north of 26° 40′ N (Doyle and Holmes, 1985). Sediments are composed of biogenic carbonates that grade from coarse grained (foraminifera, pteropods, and larger carbonate-based fragments) to fine grained (coccolithofore and foraminifera ooze) with increasing depth (Mullins et al., 1988a; Gardulski et al., 1990). The sediment overlay in this depth zone is often thin or lacking (minimal around 525 m), potentially a result of periodic interaction of the LC with the upper slope (Doyle and Holmes, 1985). Mass wasting also moves sediments westward from the WFS toward the deeper Florida Escarpment (Brooks and Holmes, 2011). Many of the WFS coral mounds and surroundings are superficially similar to those in the same depth range on the Campeche Bank (Hebbeln et al., 2014). The combination of rocky ledges and scarps mixed with putative L. *pertusa* bioherms on the WFS also resembles habitats in the same depth ranges in the Atlantic Ocean off Jacksonville, FL, where numerous ledges and bioherm-like structures were documented (Paull et al., 2000; Reed et al., 2006; Partyka et al., 2007; Ross et al., 2015). It is unclear whether underlying geological differences influence DSC development, but the general patterns of development throughout the GOM are similar: DSC colonization of various hard substrata and in some places, with appropriate currents and sedimentary regimes, subsequent formation of elevated bioherms. In the GOM and elsewhere, the exposure of various hard substrata and the build-up of coral bioherms appears to be facilitated by strong currents (i.e., Loop Current, Gulf Stream) (Doyle and Holmes, 1985; Paull et al., 2000).

The prominent long rocky scarp that defines the eastern portion of this study area is a Miocene-aged outcropping of phosphorites formed and maintained by LC erosion (when the LC swings inshore or in prior geological eras) (Doyle and Holmes, 1985; Mullins et al., 1988a; Holmes, 1981). Our description of the scarp agrees with previous reports (scarp profiles of 32–38 m) (Lindberg and Lockhart, 1993; Reed et al., 2006; Hübscher et al., 2010). Hübscher et al. (2010) noted a moat channel at the base of the scarp (same area as our southernmost dives), a feature also apparent in most of our sonar data. The northern extent to which we mapped the scarp was 26° 30′ N, but Newton et al. (1987) illustrated it to about 27° 10′ N. Although not completely mapped and perhaps buried or partially buried in places, the scarp may be continuous at depths of 250–500 m from off west-central Florida south to the Florida Keys where it may join a similar feature identified in Lidz et al. (2006). In depths below 300 m, this extensive hardground scarp represents a substantial potential substratum for DSC, other sessile invertebrates, and their associates.

Numerous mounds and ridges occurred west of the scarp in the 400–600 m depth zone. These outcrops, likely once part of the scarp, were interpreted as Pleistocene aged hardgrounds composed of calcarenites and phosphatic limestone likely resulting from past erosion by the LC (Newton et al., 1987; Mullins et al., 1988a, 1988b). Hübscher et al. (2010) suggested that one of the ridges that we examined may have resulted from mass wasting (from the scarp) and that mounded sediments at the base of the scarp may be contourite drifts formed by north flowing bottom currents. Over 900 mounds and ridges were counted within the northern part of the study area (parts of Fig. 3 mapped with multibeam sonar between the 400–700 m contours), and many more likely occur to the south, but this area was less well mapped. Because our methods for identifying mounds were conservative ($\geq$14° slopes, limits to sonar resolution), there are probably many smaller hardground or DSC structures within this region.

These mounds and ridges provide abundant attachment sites for DSC, which are dominated by L. *pertusa*. DSC mounds on the WFS were first reported to range over approximately 20 km along the 500 m isobath and include mostly dead colonial scleractinians (Newton et al., 1987). From a single video transect across a mound in the same area as Newton et al. (1987), Reed et al. (2006) observed a terraced structure and up to 20% living *L. pertusa* coverage on the mound top, noting that most live coral was on the northeast face. Hübscher et al.'s (2010) north-south camera transect (overlapping some of our southern-most dives) documented a variety of bottom types, including mounds formed by stacked boulders colonized by living and dead *L. pertusa* and other DSC. Contrary to Reed et al. (2006), they reported DSCs concentrated on the southern flanks of the mounds, facing a predicted north-flowing bottom current. These limited transects across a few mounds were not adequate to determine WFS coral distributions. Our multibeam sonar and visual observations indicated DSC concentrations occurred over a much larger area than previously reported, and the DSC covered all sides and tops of several major mound/ridge clusters. Patterns in directionality of concentrations of living or dead *L. pertusa* could not be resolved, and most of the living DSCs were consistently observed on and near the tops of features, with most living corals usually shallower than about 525 m.

We maintain that some mounds along the WFS are in various stages of bioherm formation (see Roberts et al., 2009), with the existing rocky boulders forming the original coral attachment substrata. Based on stacked hyperbolae seismic reflections and limited visual observations, Hübscher et al. (2010) concluded that the WFS mounds were not coral-built, but that corals only colonized existing hard substrata. Although true that corals colonize the hardgrounds, the role of *L. pertusa* in WFS mound construction requires further consideration. In many DSC areas in the GOM, off the SEUS, and in other regions, multiple stacked reflection hyperbolae (for examples see Mienis et al., 2006; Ross and Nizinski, 2007) were characteristic of putative coral bioherms. In most cases visual observation of those mounds did not reveal exposed rocky formations (although some may have been buried within the mounds), but they appeared to be complexes of unconsolidated sediments and coral rubble, capped with living and/or dead coral. The upper portions of many of the structures on the WFS (west of the scarp) exhibited this same coral and sediment matrix as observed elsewhere, the major difference being that boulders occurred in places, especially along the bases of mounds. Although rocky components are more prominent on the WFS compared with some DSC ecosystems outside the GOM, visual data suggested that at least parts of these mounds are biogenic. If corals continue to grow and entrap sediment, the rocky components may eventually be buried completely.

In summary, the portion of the WFS examined in this study is oceanographically dynamic and geologically complex. The interplay of hard substrata outcrops with strong currents and upwelling probably encouraged the development and maintenance of extensive DSC communities. Assuming that all or most of the corals were dead, Newton et al. (1987) proposed that the WFS mounds represented extinct or relict systems; however, their hypotheses were hampered by limited data, especially on the abundant living DSC on the WFS. Our data suggest that the area of DSC (especially scleractinians) and deep-reef habitat is more extensive along the WFS than elsewhere in the

GOM, although Campeche Bank should be further explored. This is particularly striking, given that DSC ecosystems in the northern GOM have been more extensively mapped and studied over the last 12 years, while most of the WFS hardgrounds are unexplored. Thus, the extent of DSC on the WFS is likely much larger than documented here. Considering that deep-coral habitat models tend to overpredict habitat suitability (Davies and Guinotte, 2011; Georgian et al., 2014), such models suggested much more DSC habitat at the VK sites (Georgian et al., 2014) than we noted (S1 Fig.), but the areas of highest coral concentrations coincided with our observations for VK sites. A DSC area on Campeche Bank was recently reported to be at least 40 km^2, larger than any such biotope yet documented in the GOM, but the exact area included was unclear (Hebbeln et al., 2014). Our intensively surveyed parts of the WFS exhibiting high DSC accumulations totaled 1.727 km^2 (black boxes, S1 Fig.), but if the area surveyed by multibeam sonar that includes the scarp and other topographic highs is included, the DSC and deep reef province of the WFS is at least 157 km^2 (blue boxes, S1 Fig.). Additional multibeam sonar mapping coupled with sub-bottom profiling, bottom coring, oceanographic information and visual surveys are needed to better understand the complex WFS and the processes influencing DSC accumulations. More extensive and varied explorations of the WFS will benefit habitat and associated community management, especially considering possible expansions of bottom fisheries and energy industry activities into deeper water. Conservation strategies similar to those undertaken for DSC ecosystems off the SEUS (Martin, 2015) and along the US middle Atlantic (see https://www.greateratlantic.fisheries.noaa.gov/stories/2016/september/26_deepsea_corals_in_the_mid-atlantic.html, 2016), are being considered by the Gulf of Mexico Fishery Management Council to ensure the long term integrity of the DSC and rocky deep reefs of the GOM.

Author Contributions

Conceived of the study, was Chief Scientist on 3 cruises and co-led one cruise: SWR. Directed and conducted most analyses, including data management: MR, SWR. Participated in cruises: SWR, MR, SDB. Co-Chief Scientist on one cruise, assisted with data collection, reviewed coral data: SDB. Wrote the paper: SWR, MR. Reviewed and edited manuscript drafts: SDB, MR.

Acknowledgments

We thank Dr. G. Brewer (formerly USGS) for support and assistance during the project. We thank all cruise science personnel for their hard work at sea and in dealing with logistics and data before and after the cruises. The encouragement and support of G. Boland (BOEM) during these studies is appreciated. We thank S. Cairns and D. Opresko for help with DSC identifications. D. Naar and E. Cordes generously provided multibeam data collected at WFS (*Lost Coast Explorer*) and VK sites (NOAA ship *Nancy Foster*). M. Partyka assisted with multibeam operations on the *Nancy Foster*. We thank the ship and shore based personnel who operated the R/V *Seward Johnson*, R/V *Cape Hatteras*, NOAA ship *Nancy Foster*, NOAA ship *Ronald H. Brown,* NOAA ship *Okeanos Explorer*, and *Lost Coast Explorer* for their assistance during the cruises. Our thanks to W. Jaap for constructive comments on this manuscript. Finally, we thank the personnel of the *Johnson-Sea-Link II*, *Kraken II*, and *Jason II* for exemplary service during the missions.

Appendix A. Supporting information

Supplementary data associated with this article can be found in the online version at doi:10.1016/j.dsr.2016.12.005.

References

Behringer, D.W., Molinari, R.L., Festa, J.F., 1977. The variability of anticyclonic current patterns in the Gulf of Mexico. J. Geophys. Res. 82, 5469–5476.
Bouma, A.H., Roberts, H.H., 1990. Northern Gulf of Mexico continental slope. Geo-Mar. Lett. 10, 177–181.
Brooke, S., Schroeder, W.W., 2007. State of deep coral ecosystems in the Gulf of Mexico region: Texas to the Florida Straits. In: Lumsden, S.E., Hourigan, T.F., Bruckner, A.W., Dorr, G. (Eds.), The State of Deep Coral Ecosystems of the United States. NOAA Technical Memorandum CRCP-3, Silver Spring, MD, 271–306.
Brooke, S., Holmes, M.W., Young, C.M., 2009. Sediment tolerance of two different morphotypes of the deep-sea coral *Lophelia pertusa* from the Gulf of Mexico. Mar. Ecol. Prog. Ser. 390, 137–144.
Brooke, S.D., 2016. Reproductive biology of deep-sea corals. In: Demopoulos, A.W.J., Ross, S.W., Kellogg, C.A., Morrison, C.L., et al. (Eds.), Deepwater Program: Lophelia II Continuing Ecological Research on Deep-Sea Corals and Deep Reef Habitats in the Gulf of Mexico (Chapter 10). U.S. Department of the Interior, U.S. Geological Survey Report Series (in press)
Brooks, G.R., Holmes, C.W., 2011. West Florida continental slope. In: Buster, N.A., Holmes, C.W. (Eds.), Gulf of Mexico Origin, Waters, and Biota Vol. 3. Geology. Texas A & M Univ. Press, College Station, 129–139.
Brooks, J.M., Fisher, C., Cordes, E., Baums, I., Bernard, B., Church, R., Etnoyer, P., German, C., Goehring, E., McDonald, I., Roberts, H., Shank, T., Warren, D., Welsh, S., Wolff, G., Weaver, D., 2015. Exploration and research of northern Gulf of Mexico deepwater natural and artificial hard-bottom habitats with emphasis on coral communities: reefs, rigs, and wrecks-"*Lophelia* II." (Final report). U.S. Dept. of the Interior, Bureau of Ocean Energy Management, Gulf of Mexico OCS Region, New Orleans, LA., 628.
Candela, J., Sheinbaum, J., Ochoa, J., Badan, A., 2002. The potential vorticity flux through the Yucatan Channel and the Loop Current in the Gulf of Mexico. Geophys. Res. Lett. 29, 16–1-16-4.
Continental Shelf Associates, 2007. Characterization of northern Gulf of Mexico deepwater hard bottom communities with emphasis on *Lophelia* coral. US Department of the Interior, Minerals Management Service, Gulf of Mexico OCS Region, New Orleans, LA OCS Study MMS 2007–044, 169, (appendices).
Cordes, E.E., McGinley, M.P., Podowski, E.L., Becker, E.L., Lessard-Pilon, S., Viada, S.T., Fisher, C.R., 2008. Coral communities of the deep Gulf of Mexico. Deep-Sea Res. I 55, 777–787.
Davies, A.J., Duineveld, G.C.A., van Weering, T.C.E., Mienis, F., Quattrini, A.M., Seim, H.E., Bane, J.M., Ross, S.W., 2010. Short-term environmental variability in cold-water coral habitat at Viosca Knoll, Gulf of Mexico. Deep-Sea Res. I 57, 199–212.
Davies, A.J., Guinotte, J.M., 2011. Global habitat suitability for framework-forming cold-water corals. Plos One 6, e18483.
Dodds, L.A., Roberts, J.M., Taylor, A.C., Marubini, F., 2007. The cold-water coral *Lophelia pertusa* (Scleractinia) reveals metabolic tolerance to temperature and dissolved oxygen change. J. Exp. Mar. Biol. Ecol. 349, 205–214.
Doyle, L.J., Holmes, C.W., 1985. Shallow structure, stratigraphy, and carbonate sedimentary processes of West Florida upper continental slope. Am. Assoc. Pet. Geol. Bull. 69, 1133–1144.
Gardulski, A.F., Mullins, H.T., Weiterman, S., 1990. Carbonate mineral cycles generated by foraminiferal and pteropod response to Pleistocene climate: west Florida ramp slope. Sedimentology 37, 727–743.
Georgian, S.E., Shedd, W., Cordes, E.E., 2014. High-resolution ecological niche modelling of the cold-water coral *Lophelia pertusa* in the Gulf of Mexico. Mar. Ecol. Prog. Ser. 506, 145–161.
Hall-Spencer, J., Rogers, A., Davies, J., Foggo, A., 2007. Deep-sea coral distribution on seamounts, oceanic islands, and continental slopes in the northeast Atlantic. In: George, R.Y., Cairns, S.D. (Eds.), Conservation and Adaptive Management of Seamount and Deep-sea Coral Ecosystems. University of Miami, 135–146.
Hamilton, P., 1990. Deep currents in the Gulf of Mexico. J. Phys. Oceanogr. 20, 1087–1104.
He, R., Weisberg, R.H., 2003. A Loop Current intrusion case study on the West Florida shelf. J. Phys. Oceanogr. 33, 465–477.
Hebbeln, D., Wienberg, C., Wintersteller, P., Freiwald, A., Becker, M., et al., 2014. Environmental forcing of the Campeche cold-water coral province, southern Gulf of Mexico. Biogeosciences 11, 1799–1815.
Holmes, C.W., 1981. Late Neogene and Quaternary geology of the southwestern Florida shelf and slope. US Department of the Interior Geological Survey, (Open-File Rept 81-1029).
Hübscher, C., Dullo, C., Flögel, S., Titschack, J., Schönfeld, J., 2010. Contourite drift evolution and related coral growth in the eastern Gulf of Mexico and its gateways. Int. J. Earth Sci. 99, 191–206.
International Hydrographic Organization, 2013. Standardization of undersea feature names: guidelines, proposal form, terminology (ed. 4.1.0, Publication No. B-6). International Hydrographic Organization, Monaco, 38.
Jochens, A.E., DiMarco, S.F., 2008. Physical oceanographic conditions in the deepwater Gulf of Mexico in summer 2000–2002. Deep-Sea Res. II 55, 2541–2554.
Larsson, A.I., Järnegren, J., Strömberg, S.M., Dahl, M.P., Lundälv, T., Brooke, S.D., 2014. Embryogenesis and larval biology of the cold-water coral *Lophelia pertusa*. Plos One 9 (7), e102222.
Lessard-Pilon, S.A., Podowski, E.L., Cordes, E.E., Fisher, C.R., 2010. Megafauna community composition associated with *Lophelia pertusa* colonies in the Gulf of Mexico. Deep-Sea Res. II 57, 1882–1890.
Lidz, B.H., Reich, C.D., Peterson, R.L., Shinn, E.A., 2006. New maps, new information: coral reefs of the Florida keys. J. Coast. Res. 22, 260–282.

Lindberg, W.J., Lockhart, F.D., 1993. Depth-stratified population structure of geryonid crabs in the eastern Gulf of Mexico. J. Crustace. Biol. 13, 713–722.
Liu, Y., Weisberg, R.H., Hu, C., Kovach, C., Riethmüller, R., 2011. Evolution of the Loop Current system during the Deepwater Horizon oil spill event as observed with drifters and satellites. In: Liu, Y. (Ed.), Monitoring and Modeling the Deepwater Horizon Oil Spill: A Record-Breaking Enterprise. Geophysical Monographs Series 195. American Geophysical Union, Washington, D.C., 91–101.
Lunden, J.J., McNicholl, C.G., Sears, C.R., Morrison, C.L., Cordes, E.E., 2014. Acute survivorship of the deep-sea coral *Lophelia pertusa* from the Gulf of Mexico under acidification, warming, and deoxygenation. Front. Mar. Sci. 1, 1–12.
Martin, A., 2015. Implementation of Coral Habitat Areas of Particular Concern (CHAPCs): South Atlantic Fishery Management Council process. In: Bortone, S.A. (Ed.), Interrelationships Between Corals and Fisheries. CRC Marine Biology Series No 16. CRC Press, Boca Raton, FL, 39–50.
Maul, G.A., Vukovich, F.M., 1993. The relationship between variations in the Gulf of Mexico Loop Current and Straits of Florida volume transport. J. Phys. Oceanogr. 23, 785–796.
Mienis, F., Van Weering, T., De Haas, H., De Stigter, H., Huvenne, V., Wheeler, A., 2006. Carbonate mound development at the SW Rockall Trough margin based on high resolution TOBI and seismic recording. Mar. Geol. 233, 1–19.
Mienis, F., Duineveld, G.C.A., Davies, A.J., Ross, S.W., Seim, H., Bane, J., van Weering, T.C.E., 2012. The influence of near-bed hydrodynamic conditions on cold-water corals in the Viosca Knoll area, Gulf of Mexico. Deep-Sea Res. I 60, 32–45.
Molinari, R.L., 1980. Current variability and its relation to sea-surface topography in the Caribbean Sea and Gulf of Mexico. Mar. Geod. 3, 409–436.
Molinari, R.L., Mayer, D.A., 1982. Current meter observations on the continental slope at two sites in the eastern Gulf of Mexico. J. Phys. Oceanogr. 12, 1480–1492.
Molinari, R.L., Morrison, J., 1988. The separation of the Yucatan Current from the Campeche Bank and the intrusion of the Loop Current into the Gulf of Mexico. J. Geophys. Res. 93, 10645–10654.
Morrison, C.L., Ross, S.W., Nizinski, M.S., Brooke, S., Järnegren, J., Waller, R.G., Johnson, R.L., King, T.L., 2011. Genetic discontinuity among regional populations of *Lophelia pertusa* in the North Atlantic Ocean. Conserv. Genet. 12, 713–729.
Mullins, H.T., Gardulski, A.F., Hinchey, E.J., Hine, A.C., 1988a. The modern carbonate ramp of central West Florida. J. Sediment. Petrol. 58, 273–290.
Mullins, H.T., Gardulski, A.F., Hine, A.C., Melillo, A.J., Wise, S.W., Jr., Applegate, J., 1988b. Three-dimensional sedimentary framework of the carbonate ramp slope of central west Florida: a sequential seismic stratigraphic perspective. Geol. Soc. Am. Bull. 100, 514–533.
Newton, C.R., Mullins, H.T., Gardulski, A.F., Hine, A.C., Dix, G.R., 1987. Coral mounds on the West Florida slope: unanswered questions regarding the development of deep-water banks. Palaios 2, 359–367.
Paluszkiewicz, T., Atkinson, L.P., Posmentier, E.S., McClain, C.R., 1983. Observations of a Loop Current frontal eddy intrusion onto the West Florida Shelf. J. Geophys. Res. 88, 9639–9651.
Partyka, M.L., Ross, S.W., Quattrini, A.M., Sedberry, G.R., Birdsong, T.W., Potter, J., 2007. Southeastern United States deep sea corals (SEADESC) initiative: a collaborative effort to characterize areas of habitat-forming deep-sea corals. NOAA Technical Memorandum OAR OER 1, Silver Spring, MD, 176.
Paull, C.K., Neumann, A.C., am Ende, B.A., Ussler, W., III, Rodriguez, N.M., 2000. Lithoherms on the Florida-Hatteras slope. Mar. Geol. 166, 83–101.
Quattrini, A.M., Ross, S.W., Carlson, M.C.T., Nizinski, M.S., 2012. Megafaunal-habitat associations at a deep-sea coral mound off North Carolina, USA. Mar. Biol. 159, 1079–1094.
Quattrini, A.M., Etnoyer, P.J., Doughty, C., English, L., Falco, R., Remon, N., Rittinghouse, M., Cordes, E.E., 2014. A phylogenetic approach to octocorals community structure in the deep Gulf of Mexico. Deep-Sea Res. II 99, 92–102.
Reed, J.K., Weaver, D.C., Pomponi, S.A., 2006. Habitat and fauna of deep-water *Lophelia pertusa* coral reefs off the southeastern U.S.: Blake Plateau, Straits of Florida, and Gulf of Mexico. Bull. Mar. Sci. 78, 343–375.
Reed, J.K., Messing, C., Walker, B.K., Brooke, S., Correa, T.B.S., Brouwer, M., et al., 2013. Habitat characterization, distribution, and areal extent of deep-sea coral ecosystems off Florida, southeastern U.S.A. Caribb. J. Sci. 47, 13–30.
Roberts, H., 2011. Surficial geology of the northern Gulf of Mexico continental slope. In: Buster, N.A., Holmes, C.W. (Eds.), Gulf of Mexico Origin, Waters, and Biota 3. Geology. Texas A & M Univ. Press, College Station, 209–228.
Roberts, J.M., Wheeler, A.J., Freiwald, A., Cairns, S.D., 2009. Coldwater corals: the biology and geology of deep-sea coral habitats. Cambridge University Press, Cambridge, 352.
Ross, S.W., Nizinski, M.S., 2007. State of deep coral ecosystems in the U.S. southeast region: Cape Hatteras to southeastern Florida. In: Lumsden, S.E., Hourigan, T.F., Bruckner, A.W., Dorr, G. (Eds.), The State of Deep Coral Ecosystems of the United States. NOAA Technical Memorandum CRCP-3 Silver Spring MD, 233–270.
Ross, S.W., Quattrini, A.M., 2007. The fish fauna associated with deep coral banks off the southeastern United States. Deep-Sea Res. I 54, 975–1007.
Ross, S.W., Quattrini, A.M., Roa-Varón, A.Y., McClain, J.P., 2010. Species composition and distributions of mesopelagic fishes over the slope of the north-central Gulf of Mexico. Deep-Sea Res. II 57, 1926–1956.
Ross, S.W., Demopoulos, A.W.J., Kellogg, C.A., Morrison, C.L., Nizinski, M.S., Ames, C. L., Casazza, T.L., Gualtieri, D., Kovacs, K., McClain, J.P., Quattrini, A.M., Roa-Varón, A.Y., Thaler, A.D., 2012. Deepwater Program: Studies of Gulf of Mexico Lower Continental Slope Communities Related to Chemosynthetic and Hard Substrate Habitats. US Geological Survey Open-File Rept.2012-1032, 301pp.
Ross, S.W., Brooke, S., Quattrini, A., Rhode, M., Watterson, J.C., 2015. A deep-sea community, including *Lophelia pertusa*, at unusually shallow depths in the Western North Atlantic Ocean off northeastern Florida. Mar. Biol. 162, 635–648.
Schroeder, W.W., Brooke, S.D., Olson, J.B., Phaneuf, B., McDonough, J.J., III, Etnoyer, P., 2005. Occurrence of deep-water *Lophelia pertusa* and *Madrepora oculata* in the Gulf of Mexico. In: Freiwald, A., Roberts, J.M. (Eds.), Cold-water Corals and Ecosystems.. Springer, 297–307.
Schroeder, W.W., Brooke, S.D., 2011. Habitat-forming deepwater scleractinian corals in the Gulf of Mexico. In: Buster, N.A., Holmes, C.W. (Eds.), Gulf of Mexico Origin, Waters, and Biota 3. Geology. Texas A & M Press, College Station, TX., 355–363.
Vukovich, F.M., Maul, G.A., 1985. Cyclonic eddies in the eastern Gulf of Mexico. J. Phys. Oceanogr. 15, 105–117.
Young, C.M., He, R., Emlet, R.B., Li, Y., Qian, H., Arellano, S.M., Van Gaest, A., Bennett, K.C., Wolf, M., Smart, T.I., Rice, M.E., 2012. Dispersal of deep-sea larvae from the Intra-American Seas: simulations of trajectories using ocean models. Int. Comp. Biol. 52, 483–496.